

# Arm-hand motion-force coordination for physical interactions with non-flat surfaces using dynamical systems: Toward compliant robotic massage

Mahdi Khoramshahi<sup>1\*</sup>, Gustav Henriks<sup>1</sup>, Aileen Naef<sup>1</sup>, Seyed Sina Mirrazavi Salehian<sup>1</sup>, Joonyoung Kim<sup>2</sup>, and Aude Billard<sup>1</sup>

**Abstract**—Many manipulation tasks require coordinated motions for arm and fingers. Complexity increases when the task requires to control for the force at contact against a non-flat surface; This becomes even more challenging when this contact is done on a human. All these challenges are regrouped when one, for instance, massages a human limb. When massaging, the robotic arm is required to continuously adapt its orientation and distance to the limb while the robot fingers exert desired patterns of forces and motion on the skin surface. To address these challenges, we adopt a Dynamical System (DS) approach that offers a unified motion-force control approach and enables to easily coordinate multiple degrees of freedom. As each human limb may slightly differ, we learn a model of the surface using support vector regression (SVR) which enable us to obtain a distance-to-surface mapping. The gradient of this mapping, along with the DS, generates the desired motions for the interaction with the surface. A DS-based impedance control for the robotic fingers allows to control separately for force along the normal direction of the surface while moving in the tangential plane. We validate our approach using the KUKA IIWA robotic arm and Allegro robotic hand for massaging a mannequin arm covered with a skin-like material. We show that our approach allows for 1) reactive motion planning to reach for an unknown surface, 2) following desired motion patterns on the surface, and 3) exerting desired interaction forces profiles. Our results show the effectiveness of our approach; especially the robustness toward uncertainties for shape and the given location of the surface.

## I. INTRODUCTION

Body massage is among the most effective and widely accessible means to recover from physical fatigue, and a reliable means of occupational diseases prevention [1]. Therefore, it comes as no surprise that robotic systems have been developed to try to recreate these benefits by mimicking human massage patterns [2]. While there exist several automated massage platforms on the market [3–8], they are mainly limited to massaging the back and provide very simple mechanical and repetitive movements. Massage is a challenging task as it requires reactive and coordinated arm-finger motion planning, safe and compliant interaction as the robot is in direct contact with the human. Force exerted on the skin using robotic fingers must vary following specific patterns. The whole must be adaptive to be applied to the variety of human limb surfaces. Therefore, in order to realize effective and comfortable massage actions amenable to a

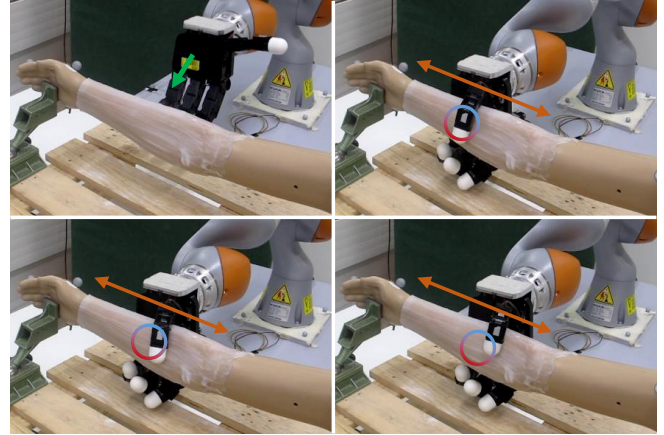


Fig. 1: Robotic arm-hand setup for a massaging application. The robot reaches the mannequin arm, moves back and forth along it and performs massaging pattern using the thumb varying the applied forces; i.e., high/low forces indicated by red/blue circle.

wide range of end-users, several challenges in motion and force control and surface modeling must be overcome.

Force control is an essential part of robotic system meant to interact with objects and humans. Recent progresses have shown the benefits of implicit force control (i.e., impedance control [9]) over direct and explicit methods. By considering the interaction dynamics (with possible disturbances and uncertainties), impedance control approaches provide robust and stable interaction with surfaces [10,11]. They ensure that the interaction is safer and offer compliance during task execution. When combined with dynamical systems for trajectory generation, impedance control law provides a natural adaptation of the motion pattern to the surface movement [12]. It can also enable compliant and robust control of motion and force simultaneously under surface movement [13–15]. In our previous work [15], we only considered interaction with surfaces using a robotic arm equipped with a finger tool; i.e., a rigid non-actuated cylindrical shape tool with a round tip to apply desired forces to surfaces. However, many robotic tasks (such as massaging) require dexterous manipulation where the robotic hand manipulates surfaces and objects. For this purpose, in this work, we tackle the problem to control for force exerted by fingers mounted on a robotic hands in addition to controlling for compliant arm

<sup>1</sup> Learning Algorithm and Systems Laboratory, EPFL, Switzerland

<sup>2</sup> Samsung Research, South Korea

\*Corresponding author: mahdi.khoramshahi@epfl.ch

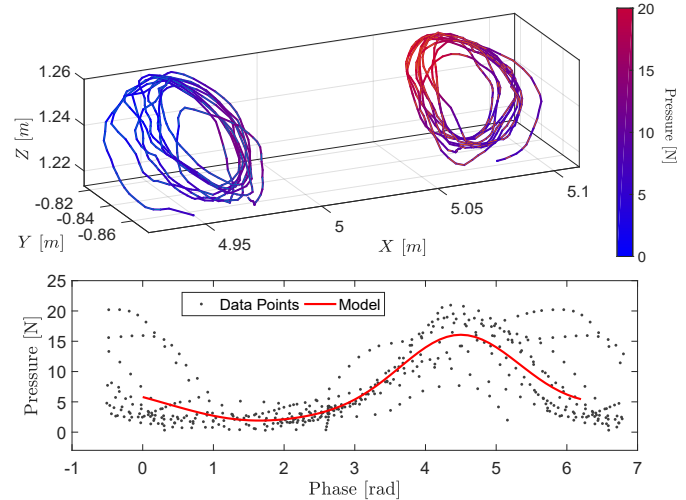


Fig. 2: (**left**) Our experimental setup to record the expert’s motions and forces during a massaging session for arm and back/shoulder. OptiTrack markers are used to track the motion pattern and FingerTPS sensors are used to record the pressure data. (**right**) Extracted motion-force patterns (from back/shoulder massage) for the thumbs which resemble a circular behavior with applied pressured linked to the phase of the motion. Arm massage follows a similar pattern. It should be noted that force and pressure are used interchangeably in this work since the FingerTPS system measures an average of the force applied across the entire sensor surface; i.e., choosing  $N$  as the pressure unit in FingerTPS software.

movement to remain in contact with the surface.

Compliance for robot hands has been investigated extensively to offer more robust grasps; see [16,17] for using soft materials, [18] compliant mechanism at the fingertip, [19–21] variable stiffness, and [22] Cartesian impedance control. Such compliant mechanisms regulate the interaction forces during the grasping and provide adaptable behavior toward the environment with minimal control effort. However, manipulation tasks (i.e., other than grasping) require algorithms and control strategies for active compliant behavior to generate a desired motion-force behavior toward an object/surface. To achieve this, we use dynamical system-based control framework where the physical interaction with the environment can be learned from demonstrations. Dynamical systems (DS) are effective tools to embed motion dynamics that resemble human dynamics and can be trained from human demonstrations [23]. This is advantageous when the task is required to be performed in a human-like manner; see [24,25] for human-like handover, [26] for obstacle avoidance during reaching tasks, [27] for grasping, and [28,29] for manipulation tasks. For the massaging task, such approach is feasible when motion and force pattern can be learned from expert therapist; see [30,31] for learning the force patterns during shoulder massage, [32] for learning Chinese massage therapy, and [33] for reproducing path and forces of a skilled physician. Here, we exploit these concepts and show how motion and force demonstrated by a therapist can be embedded in a dynamical system’s framework and executed on a robotic arm-hand system; see Fig. 1.

For robotic surface/object manipulation, task representation is one of the main challenges. On the other hand, for reaching tasks, representing the goal of the reaching motion as the attractor of a state-dependent dynamical system proves

to be efficient.

One reason for this efficiency is that such dynamics operate on a normalized vector space where the robot reduces its distance toward the goal through the desired dynamics. However, regarding surface and object manipulation, object or surface-oriented dynamics approach is less explored; i.e., having a distance function (from any arbitrary point in the space to the object/surface) which allows for motion planning for the robotic arm, hand, and fingers. Machine learning techniques such as SVR and GPR have been used to model the object surfaces and the distance to a surface [34,35]. In this work, we use such mapping to control the robotic arm to position the hand at a desired distance and orientation with respect to the surface. Moreover, this mapping is used to control the fingers to apply the force in the normal direction and track the desired motions in the tangential plane as in [15].

## II. METHOD

In this section, we describe our experimental setup to record expert therapist motions and forces in a massaging scenario. Then, we present our control DS-based framework for the arm-hand system. Finally, we show how SVR is used to model a non-flat surface and to obtain a distance-to-surface mapping which is used for motion-force control.

### A. Learning from demonstrations

To reach a human-like massaging behavior, we collected demonstration from a registered massage therapist. The therapist demonstrated two types of massage; i.e., an arm massage, and a shoulder/back massage. The massage pattern and forces were recorded using the OptiTrack system [36] for motion capture, and the FingerTPS system [37] to record the forces exerted by the fingers; see Fig. 2(left). The

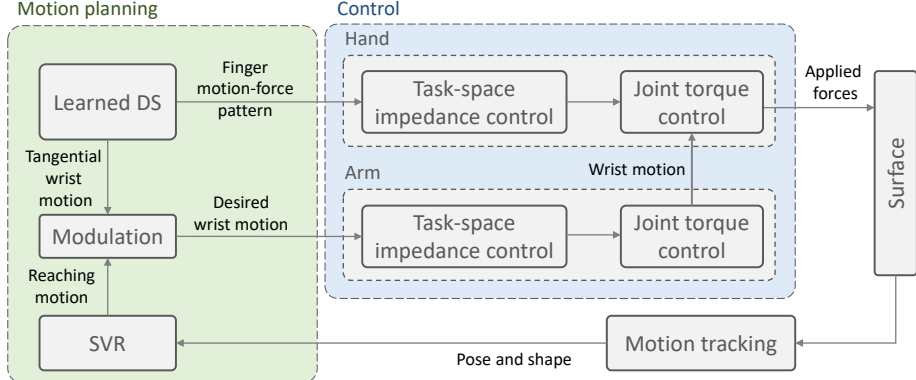


Fig. 3: The control architecture for arm-hand coordination for surface manipulation. The Dynamical System (which is learned based on human therapist demonstration) generates human-like patterns for motions and forces. The impedance control computes the necessary joint torques for the thumb to fulfill the desired behavior. The torque mode control of the finger allows for compliant interaction with the human receiving the massage. The SVR used to obtain a distance-to-surface mapping which allows to control the wrist motion in order to maintain a fixed pose relative to the surface.

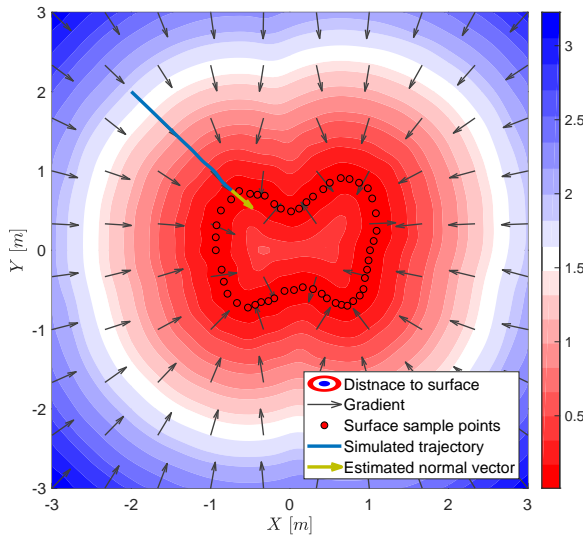


Fig. 4: Modeling a surface using Support Vector Regression. The contours represents the distance to the surface with direction of the gradient. The blue trajectory denotes a motion obtained by following the gradient where the yellow arrow represents the normal direction of surface.

OptiTrack System had a recording frequency of 120Hz, whereas the FingerTPS system had a frequency of 40Hz. Therefore, the OptiTrack data was resampled to 40Hz during pre-processing. The synchronization was done manually by starting the recordings approximately at the same time. However, there were slight adjustments made based on the appearance of a pressure signal greater than zero and visualizing the finger reaching the surface. The pressure data was also detrended to remove the drift present in the sensors. Furthermore, we adjusted the offset as to have positive values for the pressure since the thumb was always in contact with the surface. Finally, a low-pass filter with the cutoff frequency of 2Hz was applied to smooth the signal.

Fig. 2(right) shows the demonstrations in term of motion-force pattern of the thumbs. To model these patterns, we use the following Dynamical System in the polar coordinate systems.

$$\begin{cases} \dot{r} = -\alpha(r - r_0) \\ \dot{\phi} = \omega \\ F_d = g(\theta) \end{cases} \quad (1)$$

In this DS,  $r$ ,  $\theta$ , and  $\omega$  denote the radius, phase, and angular velocity respectively.  $r_0$  represents the radius of the limit-cycle. The convergence rate  $\alpha > 0$  ensures the stability of this limit-cycle. The desired contact forces  $F_d$  is computed based on the phase  $\theta$  using the function approximator  $g(\cdot)$ . Using the data collected during the demonstration, we estimate  $r_0$ ,  $\alpha$ ,  $\omega$ , and  $g(\cdot)$ . To learn  $g(\cdot)$ , we use Locally Weighted Regression with RBF kernels which is illustrated in Fig. 2(right).

Using this model, and knowing the current phase at any given moment during the movement, the force can be determined. This provides valuable insight into how a massage therapist applies forces while moving along the surface which can be translated to the robotic application.

#### B. Control of robotic arm and hand

In our architecture, both the robotic arm and the hand (i.e., the thumb) are controlled in joint-torque mode which allows for a compliant interaction with the environment; e.g., the mannequin arm for our massaging experiment. This means that the final command sent to the robot is the joint-torques. To generate the desired motions and forces for the contact task, we use our previous approach [15]. This approach is illustrated in Fig. 3 for the control of the thumb on the Allegro hand. The control objectives for the arm are:

- reach the surface and maintain a fixed relative distance/orientation
- move along the surface (i.e., mannequin arm) and maintain a desired orientation.

For the thumb, we have the following objectives:

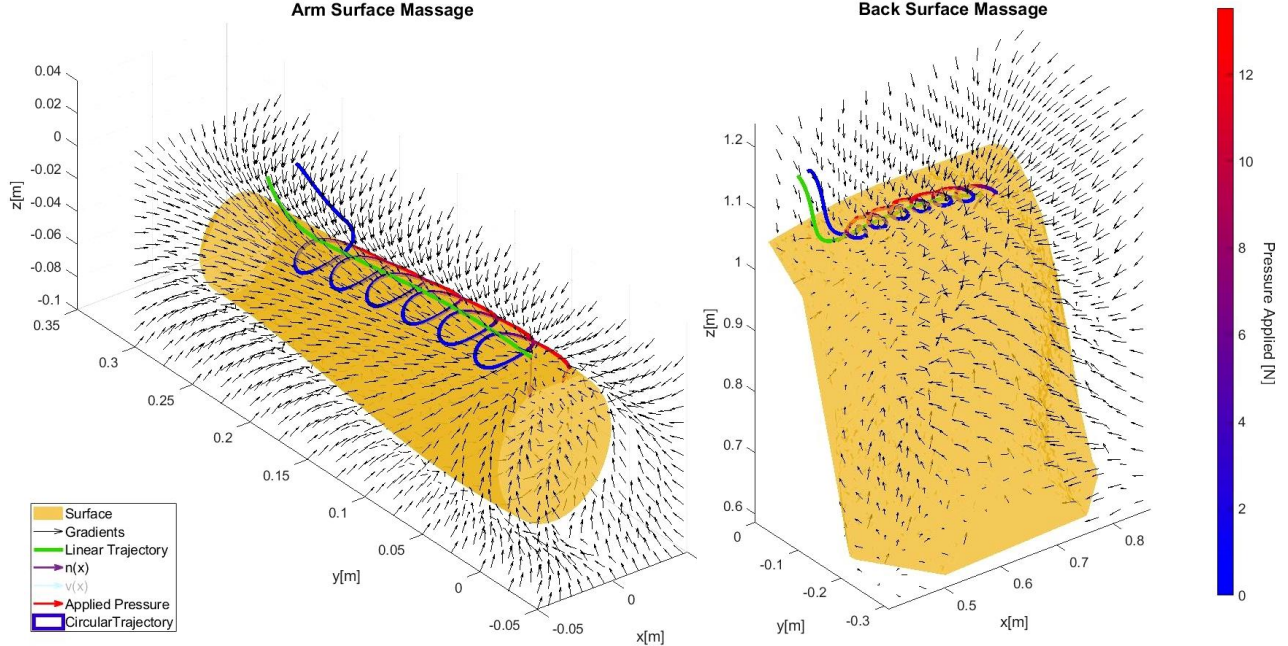


Fig. 5: Simulation of arm and back surface and massaging trajectory with force pattern overlaid. The surface was created using artificially generated data and meshed to create a smooth surface. Using the same data, and SVR model was generated and the gradient field (*black arrows*) around the surface determined. The linear trajectory (*green line*) represents how the wrist approaches the surface, and its linear progression along the surface. The circular trajectory (*red-blue line*) represents the trajectory of the thumb along the surface, implementing the circular motions of the massage. The changing color scale represents the force (N) applied to the surface through the thumb.

- follow the motion-patterns generated by Eq. 1 in the tangential plane of the surface
- exert the contact forces generated by Eq. 1 in the orthogonal direction.

We show in the next sections how modeling the surface using Support Vector Machine, along with the Dynamical Systems, enables us to reach these control objectives.

### C. Surface modeling using SVR

It is necessary to have an approximation of the distance to the surface when interacting with a surface with an arbitrary shape; especially for coordination between robotic arm and hand. For instance, the wrist of the robot should reach the surface while maintaining a safe distance while the fingers should make physical contact and exert forces in the normal direction. To obtain such mapping, we use Support Vector Regression (SVR). Having sample points from a given surface  $\mathcal{D}_s$ , we create another data-set ( $\mathcal{D}$ ) of uniformly distributed points and their distance to the nearest neighbor in  $\mathcal{D}_s$ ;  $\mathcal{D} = \{\{x, d\} \mid d = \min(\|x - x_s\|^2) \forall x_s \in \mathcal{D}_s\}$ . Then, using SVR we approximate the mapping from each point in the space ( $x$ ) to its distance to the nearest point of the surface ( $d$ ). As illustrated in Fig. 4, a distance-function is learned from a set of sample points on the surface. The gradient of this function allows the robot to reach the surface effectively. Moreover, the gradient of this function at the surface serves as an approximation for the normal vector. This allows the robot to exert forces orthogonal (or at any other arbitrary angle) to the surface.

### D. Motion planning using DS and SVR

Using the approach explained in the previous part, we generated a surface model for a generic human/mannequin arm and back illustrated in Fig. 5. The green trajectory demonstrates 1) reaching to the surface and, 2) moving along it. This reference trajectory is used to control the robot's wrist. By controlling the robot wrist at a certain distance and orientation, the robot places the thumb in a proper pose w.r.t to the surface. In this proper pose, the thumb can follow the motion pattern (of Eq. 1) in the tangential plane and exert the desired contact forces in the orthogonal direction. This simulated motion-force pattern is illustrated by the colored trajectory where red parts represented higher contact forces (obtained from  $g(\cdot)$  in Eq.1).

For the linear motion along the human/mannequin arm, we use a linear dynamical system. Upon reaching the attractor, to generate back and forth motions, we relocate the attractor to the other end of the arm. During this linear motion, the gradient of the SVR model is used to maintain the wrist at a certain distance for the surface. This distance, along with orientation, is set experimentally to position the thumb in an effective configuration with respect to the surface to maximize the workspace of the thumb in the tangential plane; i.e., aligning the two y-axes and z-axis with x-axis of the mannequin arm.

Furthermore, as illustrated in Fig. 3, the position of the human/mannequin wrist and elbow is tracked using OptiTrack system. Having these two landmarks, the pose of the SVR

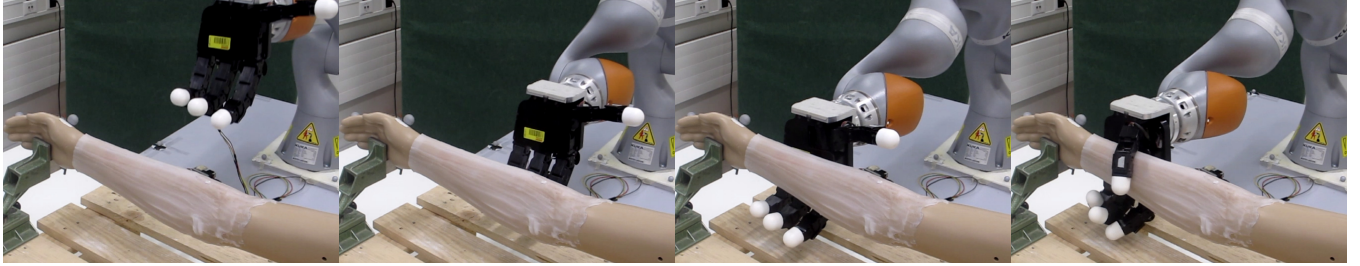


Fig. 6: Snapshots of the robotic arm and hand motion towards the mannequin arm. The robotic arm uses DS and SVR to reach the mannequin arm, where it makes contact when close enough to the arm (using the distance-to-surface function modeled by SVR).

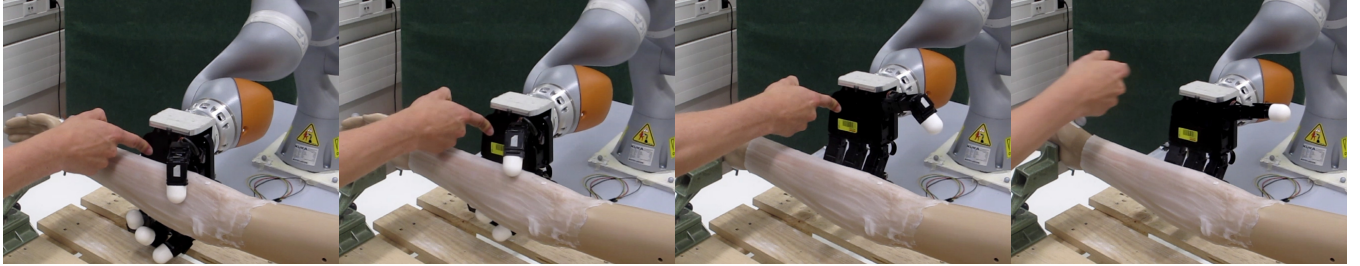


Fig. 7: Snapshots showcasing the compliance of the robotic arm. When the robotic arm is pushed away from the mannequin arm, the robotic hand opens and the robotic arm is following the direction of the push.

model is updated. The desired velocity commanded by DS (the linear motion for the arm, and the cyclic motion for the finger) are modulated using the SVR to ensure the desired contact behavior. Finally, the thumb applies the forces at the desired position on the surface. In the next section, we report on our robotic experimentation.

### III. RESULTS

#### A. Reaching motion using SVR

The pose of the mannequin arm is tracked using the OptiTrack system where markers are attached to each end. The robot then initializes its movement towards the arm by using the DS and SVR. Once it is close enough to the lower part of the arm, which is the target area of massaging, a command is sent to the hand to make contact with the surface. This can be seen in Fig. 6. At all time, the robot is compliant and can be pushed away from the arm. This opens the hand and resets its targets as seen in Fig. 7. Given the reactivity of the motion planner, the end-effector keeps its desired pose relative to the surface when the arm is moving; see Fig. 8. Such compliance and reactivity are important components for the robot control as human subjects may not be completely immobile and the robot needs to comply through different perception modalities such as vision or haptics.

#### B. Force-motion control of the thumb

Upon reaching the arm and making contact, the massaging force-motion is generated and followed; see Fig. 9. The circular motion patterns are better visible in Fig. 10 where the robot wrist is fixed. Fig. 11 shows the applied forces which depend on the phase; as computed in Eq. 1. This can

be seen in Fig. 10, where the thumb applies less force in the images with green border and more force in the images with the red border. The fingers are also compliant while performing the massage movements, which can be seen in Fig. 12.

### IV. DISCUSSION AND CONCLUSION

In this work, we proposed a framework based on Dynamical System and Support Vector Regression to perform contact tasks that require robotic arm-hand coordination. We learned the desired motion-force pattern from human demonstrations and encoded them using dynamical systems. Furthermore, we modeled the surface using SVR where the approximation of the distance to the surface and its gradient helped us with the coordinated motion planning for the robot arm and hand/finger. Using the impedance-based dynamical system approach, we delivered compliant interaction with the environment for both arm and the hand. Furthermore, this control approach allowed for motion-control (in the tangential plane) and force exertion (in the orthogonal direction) on a nonlinear surface.

In this preliminary work, our results were limited regarding tracking performance; e.g., tracking error in force and velocity commanded by Eq. 1. This was mainly due to imprecision in sensing an actuation of the Alegro hand in impedance mode. Nevertheless, our results pinpoint the importance of new designs for robotic hands in terms of actuation (larger workspace with higher torque generation), perception (to measure the applied forces to the surface), and control (to provide fast closed-loop control for impedance control). Moreover, in this work, we applied our SVR-based motion planning for a simple shape object (i.e., a mannequin

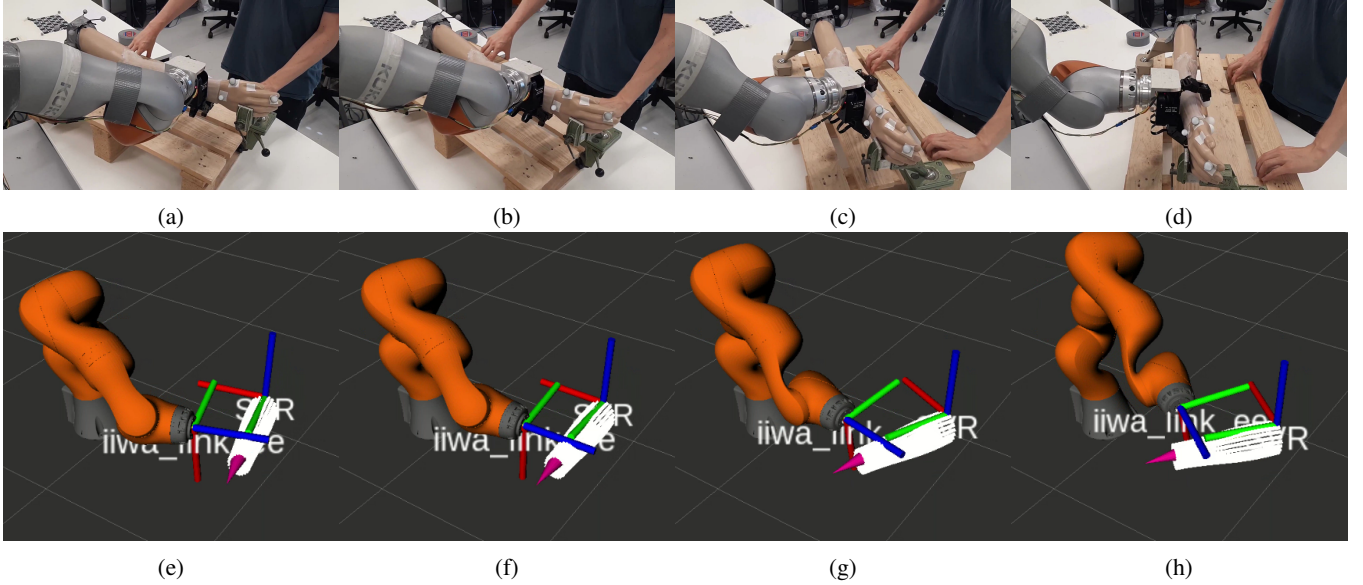


Fig. 8: Snapshots of the end-effector keeping its orientation to the surface stable while the target is rotated. (Top) Implementation during testing. (Bottom) Snapshots of visualization in RVIZ where each image (c-h) corresponds to the images in the top row (a-d).

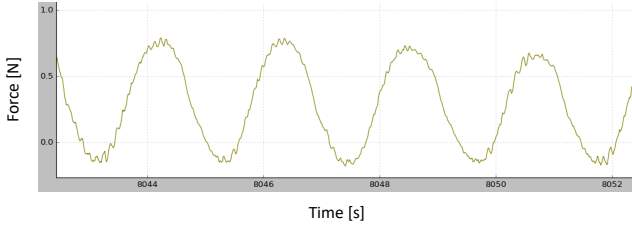


Fig. 11: The applied force during the massage using the Allegro hand thumb using the DS-based impedance control. The force increases depending on the phase of the circular dynamical system for the thumb, according to the demonstrated movements from the massage therapist.



Fig. 12: The compliance of the Allegro hand during the massage. Since the fingers are controlled in the torque mode, they remain compliant to interaction with the human receiving the massage. This behavior guarantees the safety of the interaction.

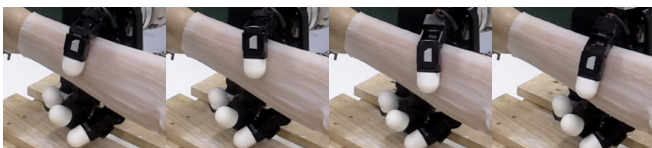


Fig. 9: Snapshots showing the massaging motion performed while the robotic arm is moving along the mannequin arm.

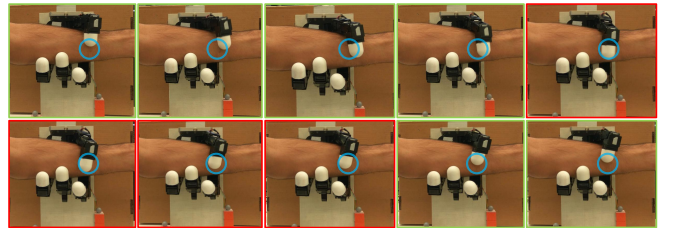


Fig. 10: The thumb is following a circular motion as indicated by the blue circle. During a part of the motion, the thumb applies the desired force necessary for the massage. The corresponding snapshots where the thumb applies the force is indicated by red frames. The snapshots with the green frame indicate the moments when the thumb applies a gentle touch to maintain the contact with arm.

arm and back). In future, we will consider more complex shapes where considering only the distance (in form of contours) is not enough for motion planning purposes.

#### ACKNOWLEDGMENT

This work received support from Samsung Research and Research and Innovation programme ICT-2014-1 under grant agreement 643950-SecondHands.

#### REFERENCES

- [1] A. Rodić and T. Borangiu, *Advances in Robot Design and Intelligent Control: Proceedings of the 25th Conference on Robotics in Alpe-Adria-Danube Region (RAAD16)*. Springer, 2016, vol. 540.
- [2] K. C. Jones and W. Du, "Development of a massage robot for medical therapy," in *Proceedings 2003 IEEE/ASME International Conference on Advanced Intelligent Mechatronics (AIM 2003)*, vol. 2. IEEE, 2003, pp. 1096–1101.
- [3] "F&P Personal Robotics, "impulse generation"," <https://www.fp-robotics.com/wp-content/uploads/2017/05/Massage-Application-2-1.pdf>, accessed: 2019-08-12.

- [4] "F&P Personal Robotics, "just for the feel of it," <https://massagerobotics.com/>, accessed: 2019-08-12.
- [5] V. Golovin, "Robot for massage," in *Proceedings of JARP, 2nd Workshop on Medical Robotics, Heidelberg, Germany*, 1997.
- [6] M. Kume, Y. Morita, Y. Yamauchi, H. Aoki, M. Yamada, and K. Tsukamoto, "Development of a mechatotherapy unit for examining the possibility of an intelligent massage robot," in *Proceedings of IEEE/RSJ International Conference on Intelligent Robots and Systems, IROS'96*, vol. 1. IEEE, 1996, pp. 346–353.
- [7] K. Mouri, K. Terashima, P. Minyong, H. Kitagawa, and T. Miyoshi, "Identification and hybrid impedance control of human skin muscle by multi-fingered robot hand," in *2007 IEEE/RSJ International Conference on Intelligent Robots and Systems*. IEEE, 2007, pp. 2895–2900.
- [8] R. C. Luo, C. P. Tsai, and K. C. Hsieh, "Robot assisted tapping control for therapeutic percussive massage applications," in *2017 IEEE International Conference on Robotics and Automation (ICRA)*. IEEE, 2017, pp. 3606–3611.
- [9] N. Hogan, "Impedance control: An approach to manipulation: Part iiimplementation," *Journal of dynamic systems, measurement, and control*, vol. 107, no. 1, pp. 8–16, 1985.
- [10] A. Albu-Schäffer, S. Haddadin, C. Ott, A. Stemmer, T. Wimböck, and G. Hirzinger, "The dlr lightweight robot: design and control concepts for robots in human environments," *Industrial Robot: an international journal*, vol. 34, no. 5, pp. 376–385, 2007.
- [11] J. Koivumäki and J. Mattila, "Stability-guaranteed force-sensorless contact force/motion control of heavy-duty hydraulic manipulators," *IEEE Transactions on Robotics*, vol. 31, no. 4, pp. 918–935, 2015.
- [12] K. Kronander and A. Billard, "Passive interaction control with dynamical systems," *IEEE Robotics and Automation Letters*, vol. 1, no. 1, pp. 106–113, 2015.
- [13] E. Shahriari, A. Kramberger, A. Gams, A. Ude, and S. Haddadin, "Adapting to contacts: Energy tanks and task energy for passivity-based dynamic movement primitives," in *2017 IEEE-RAS 17th International Conference on Humanoid Robotics (Humanoids)*. IEEE, 2017, pp. 136–142.
- [14] A. Kramberger, E. Shahriari, A. Gams, B. Nemec, A. Ude, and S. Haddadin, "Passivity based iterative learning of admittance-coupled dynamic movement primitives for interaction with changing environments," in *2018 IEEE/RSJ International Conference on Intelligent Robots and Systems (IROS)*. IEEE, 2018, pp. 6023–6028.
- [15] W. Amanhoud, M. Khoramshahi, and A. Billard, "A dynamical system approach to motion and force generation in contact tasks." *Robotics: Science and Systems (RSS)*, 2019.
- [16] R. Deimel, "Soft robotic hands for compliant grasping," Ph.D. dissertation, Technische Universität Berlin, 2017.
- [17] R. Deimel and O. Brock, "A novel type of compliant and underactuated robotic hand for dexterous grasping," *The International Journal of Robotics Research*, vol. 35, no. 1-3, pp. 161–185, 2016.
- [18] L. U. Odhner, L. P. Jentoft, M. R. Claffee, N. Corson, Y. Tenzer, R. R. Ma, M. Buehler, R. Kohout, R. D. Howe, and A. M. Dollar, "A compliant, underactuated hand for robust manipulation," *The International Journal of Robotics Research*, vol. 33, no. 5, pp. 736–752, 2014.
- [19] M. Grebenstein, M. Chalon, W. Friedl, S. Haddadin, T. Wimböck, G. Hirzinger, and R. Siegwart, "The hand of the dlr hand arm system: Designed for interaction," *The International Journal of Robotics Research*, vol. 31, no. 13, pp. 1531–1555, 2012.
- [20] S. Wolf, T. Bahls, M. Chalon, W. Friedl, M. Grebenstein, H. Höppner, M. Kühne, D. Lakatos, N. Mansfeld, M. C. Özparpucu, et al., "Soft robotics with variable stiffness actuators: Tough robots for soft human robot interaction," in *Soft robotics*. Springer, 2015, pp. 231–254.
- [21] M. Fumagalli, E. Barrett, S. Stramigioli, and R. Carloni, "Analysis of an underactuated robotic finger with variable pinch and closure grasp stiffness," in *2016 IEEE International Conference on Advanced Intelligent Mechatronics (AIM)*. IEEE, 2016, pp. 365–370.
- [22] Z. Chen, N. Y. Lii, T. Wimboeck, S. Fan, M. Jin, C. H. Borst, and H. Liu, "Experimental study on impedance control for the five-finger dexterous robot hand dlr-hit ii," in *2010 IEEE/RSJ International Conference on Intelligent Robots and Systems*. IEEE, 2010, pp. 5867–5874.
- [23] S. M. Khansari-Zadeh and A. Billard, "Learning stable nonlinear dynamical systems with gaussian mixture models," *IEEE Transactions on Robotics*, vol. 27, no. 5, pp. 943–957, 2011.
- [24] N. F. Duarte, M. Raković, and J. Santos-Victor, "Learning motor resonance in human-human and human-robot interaction with coupled dynamical system," *arXiv preprint arXiv:1905.04072*, 2019.
- [25] J. R. Medina, F. Duvallet, M. Karnam, and A. Billard, "A human-inspired controller for fluid human-robot handovers," in *2016 IEEE-RAS 16th International Conference on Humanoid Robots (Humanoids)*. IEEE, 2016, pp. 324–331.
- [26] H. Hoffmann, P. Pastor, D.-H. Park, and S. Schaal, "Biologically-inspired dynamical systems for movement generation: automatic real-time goal adaptation and obstacle avoidance," in *2009 IEEE International Conference on Robotics and Automation*. IEEE, 2009, pp. 2587–2592.
- [27] B. Moore, E. Ugur, and E. Oztop, "Biologically inspired robot grasping through human-in-the-loop robot control," 2010.
- [28] P. Kormushev, S. Calinon, and D. G. Caldwell, "Robot motor skill coordination with em-based reinforcement learning," in *2010 IEEE/RSJ international conference on intelligent robots and systems*. IEEE, 2010, pp. 3232–3237.
- [29] M. Tamasiunaite, B. Nemec, A. Ude, and F. Wörgötter, "Learning to pour with a robot arm combining goal and shape learning for dynamic movement primitives," *Robotics and Autonomous Systems*, vol. 59, no. 11, pp. 910–922, 2011.
- [30] P. Minyong, T. Miyoshi, K. Terashima, and H. Kitagawa, "Expert massage motion control by multi-fingered robot hand," in *Proceedings 2003 IEEE/RSJ International Conference on Intelligent Robots and Systems (IROS 2003)(Cat. No. 03CH37453)*, vol. 3. IEEE, 2003, pp. 3035–3040.
- [31] K. Terashima, H. Kitagawa, T. Miyoshi, P. Minyong, and T. Kondo, "Modeling and massage control of human skin muscle by using multi-fingered robot hand," *Integrated Computer-Aided Engineering*, vol. 13, no. 3, pp. 233–248, 2006.
- [32] L. Hu, Y. Wang, J. Zhang, J. Zhang, Y. Cui, L. Ma, J. Jiang, L. Fang, and B. Zhang, "A massage robot based on chinese massage therapy," *Industrial Robot: An International Journal*, vol. 40, no. 2, pp. 158–172, 2013.
- [33] V. Golovin, M. Arkhipov, and V. Zhuravlev, "Force training for position/force control of massage robots," in *New trends in medical and service robots*. Springer, 2014, pp. 95–107.
- [34] M. Li, K. Hang, D. Kragic, and A. Billard, "Dexterous grasping under shape uncertainty," *Robotics and Autonomous Systems*, vol. 75, pp. 352–364, 2016.
- [35] S. S. Mirrazavi Salehian, N. Figueroa, and A. Billard, "A unified framework for coordinated multi-arm motion planning," *The International Journal of Robotics Research*, vol. 37, no. 10, pp. 1205–1232, 2018.
- [36] "NaturalPoint, "optitrack"," <https://optitrack.com/about/careers/>, accessed: 2019-02-18.
- [37] "Pressure profile systems, fingertps sensor systems," <https://pressureprofile.com/finger-tps>, accessed: 2019-02-18.